Interleaved machine learning in application to human vascular system modeling

Elena Kornaeva
Dept. of Information Systems and Digital Technologies
Orel State University
Orel, Russia
smkornaeva@gmail.com

Alexey Kornaev
Research Center for Artificial Intelligence
Innopolis University
Innopolis, Russia
a.kornaev@innopolis.ru

Ivan Stebakov
Dept. of Mechatronics, Mechanics, and Robotics
Orel State University
Orel, Russia
chester50796@yandex.ru

Nikita Litvinenko
Research Center for Artificial Intelligence
Innopolis University
Innopolis, Russia
n.litvinenko@innopolis.university

Yuri Kazakov
Dept. of Mechatronics, Mechanics, and Robotics
Orel State University
Orel, Russia
kazakyurii@yandex.ru

Bulat Ibragimov
Dept. of Computer Science
University of Copenhagen
Copenhagen, Denmark
bulat@di.ku.dk

***Abstract*—The variational approach of finding the extremum of an objective functional is an alternative approach to the solution of partial differential equations in mechanics of continua. The great challenge in the calculus of variations direct methods is to find a set of functions that will be able to approximate the solution accurately enough. Artificial neural networks are a powerful tool for approximation, and the physics-based functional can be the natural loss for a machine learning method. In this paper, we focus on the loss that may take non-linear fluid properties and mass forces into account. We modified the energy-based variational principle and determined the constraints on its unknown functions that implement boundary conditions. We explored artificial neural networks as an option for loss minimization and the approximation of the unknown functions. We compared the obtained results with the known solutions. The proposed method allows modeling non-Newtonian fluids flow including blood, synthetic oils, paints, plastic, bulk materials, and even rheomagnetic fluids. The fluids flow velocity approximation error was up to 4% in comparison with the analytical and numerical solutions.**

***Index Terms*—physics-based machine learning, differentiable physics, loss, multilayer perceptron, convolutional neural network, continuum mechanics, calculus of variations, variational principle**

I. Introduction

The idea of taking the path of least resistance arose a long time ago, and people find its confirmation both in themselves and in the environment. Aristotle expressed this idea in his writings, Fermat used this idea to describe the law of refraction of light, and Maupertuis was the first to formulate the principle of least action in mechanics [1].

Three main approaches, given in order to increase the role of knowledge in physics, can be used when applying machine learning to physics: supervised learning, physics-informed learning, and interleaved differentiable physics and learning [2].

https://www.youtube.com/watch?v=PDeN3iCtyNY

The deep supervised learning approach helps to find complex relations in data using measurement or simulation results. For example, the convolutional neural networks (CNNs) can be trained using computational fluid dynamics (CFD) dataset to establish the relationship between the pressure on the surface of a body and the fluid flow velocity distribution around the body [3]. The combination of the CNNs and the long short-term memory (LSTM) networks demonstrates good results in studying unsteady flows [4], [5]. In spite of recent successes, the approach has low interpretability and generalization ability. Physical knowledge integration is required [6].

The physics-informed learning approach allows to train neural networks using the PDEs in their residual form as constraints in the optimisation and making them part of the loss function [2], [7], [8]. The resulting model can be discretised in space by the finite element method (FEM) and the method applies to both stationary and transient as well as linear and nonlinear PDEs [9]. A set of interesting results was obtained using relatively simple Lorenz equations instead of Navier-Stokes equations [10]–[12].

The interleaved differentiable physics and learning approach is fully based on the numerical solution of PDEs or on the minimization of a physics-based loss. The idea of approximation of unknown functions using machine learning has been known for a long time [13], [14]. A boundary value problem of solving PDEs can be transformed into the variational problem [3], [7]. An energy method based on machine learning allows to solve problem without using any data set [15]. Variational methods are usually limited in material properties, boundary

This research has been financially supported by The Analytical Center for the Government of the Russian Federation (Agreement No. 70-2021-00143 dd. 01.11.2021, IGK 000000D730321P5Q0002).

conditions, and inertial forces.

The Lagrange principle (**??**) has the following limitations:

- fluid is Newtonian;
- mass forces (for example, gravity, electromagnetic forces) are negligible;
- the unknown functions and their first derivatives are fixed on the boundary (isoperimetric statement of a variational problem);
- both, static and kinematic boundary conditions are required to find the value of the external power in **??**;
- inertial force is negligible.

Approaching the limitations above is a challenging task. The goal of the research is a new physics-based loss and its application to non-Newtoninan and rheomagnetic fluids flow modelling.

II. Related works

A. Physiological fluids flows modeling

Whole blood is a two-phase liquid, composed of cellular elements suspended in plasma. Whole blood is a non-Newtonian fluid and characterized as shear-thinning, viscoelasticity, yield stress and thixotropy behavior [16], [17]. Many experimental studies have shown that blood is a predominantly shear thinning fluid [18]–[21]. This means that blood viscosity decreases as shear rate increases. This behavior is typical for vessels of small size or in areas of stable recirculation, for example, in the venous system and parts of the arterial vasculature, where the geometry is changed and red blood cell aggregates become more stable. In different vessels, the shear rate can vary from a few 1/s to more than 1000 1/s [22], [23]. According to [17], [19] the manifestation of non-Newtonian properties of blood occurs in the range of shear rates from 1 to 200 1/s. Baskurt et al. [24] shown that blood exhibits pronounced non-Newtonian properties at shear rates up to 100 1/s, in the range from 100 to 200 1/s normal values range from 4 to 5 mPa s. When the shear rate increases above 200 1/s, the blood viscosity does not change. Works [20], [21] present viscosity measurements for blood analogues of various concentrations, it is shown that in the range of shear rates from 1 to 100 1/s, the viscosity decreases, and after 100 1/s, the viscosity is constant. Blood is also characterized by a thixotropic behavior [21], [25]. Thixotropy is more pronounced at low shear rates with a long time scale. However, this effect appears to have a less important role in blood flow than other non-Newtonian effects such as shear thinning [16], [21]. Blood also demonstrates yield stress although there is a controversy about this issue [16], [25], [26]. Yield stress models can be useful to model blood flow in capillaries where flow at very low shear rates occurs [25], [26].

A simple example of a shear thinning blood model is the power low [16], [25], for which the viscosity function is given by:

$$\mu(\xi) = \theta_0 \xi^{\theta_1 - 1}, \tag{1}$$

TABLE I: Metrics of the proposed method for the test fluid with non-Newtonian properties.

Model type	Function	Constant of model
Cross [27], [28]	$\mu_\infty + \frac{\mu_0 - \mu_\infty}{1+(\theta_0\xi)^{\theta_1}}$	$\theta_0 = 1.007$, $\theta_1 = 1.028$
Modified Cross [27], [28]	$\mu_\infty + \frac{\mu_0 - \mu_\infty}{(1+(\theta_0\xi)^{\theta_1})^{\theta}_2}$	$\theta_0 = 3.736$, $\theta_1 = 2.406$, $\theta_2 = 0.254$
Carreau-Yasuda [25], [29]	$\mu_\infty + (\mu_0 - \mu_\infty)()$	$\theta_1 = 1.902$ $\theta_1 = 1.25$ $\theta_3 = 0.22$
Eyring-Powell [16], [30]	0.1166	$\theta_1 =$ $\theta_2 =$

where θ_0, θ_1 are the model parameters; $\theta_1 < 1$ for pseudoplastic fluid; θ_0, θ_1 are different and depend on hematocrit and temperature.

The shear thinning power law model is often used for blood, due to the analytical solutions easily obtained for its governing equations, but there is a shortcoming since it predicts an unbounded viscosity at zero shear rate and zero viscosity when $\xi \to \infty$, which is unphysical [16]. Other viscosity models are shown in **??**. The asymptotic viscosities $\mu_0 = \lim_{\xi \to 0} \mu(\xi)$ and $\mu_0 = \lim_{\xi \to \infty} \mu(\xi)$, at $37°C$ and hematocrits ranging from 33–45 % are the following $\mu_0 = 0.056\ Pa{\cdot}s$ and $\mu_\infty = 0.00345\ Pa{\cdot}s$ [16].

E.Kornaeva et al. [31]

B. Physics-based machine learning

C. Network architectures

D. In-silico methods in medicine

III. Data collection

The proposed method is data set free. Meanwhile,

IV. Mathematical modeling

A. Variational formulation and the loss formalization

The paper deals with hydrodynamics. It is supposed that fluid is incompressible and the flow is laminar and steady. Since incompressibility is a natural property of fluids, the laminarity and stationarity of flows are typical assumptions in hydrodynamics [32] and in calculus of variations [1], respectively.

Some of the physical laws have variational formulation: *among all admissible functions, the proper function corresponds to the extremum value of the target functional*. In this work, it is necessary to find a kinematic function that characterizes the velocity distribution in the flow domain and minimizes a power functional.

In the previous work [33], the generalized Lagrange variational principle was proposed as the power functional for non-Newtonian fluids:

$$J_L^*[\mathbf{\Psi}] = \int_\Omega \Pi_v d\Omega \to min, \tag{2}$$

where $\mathbf{\Psi} = [\psi_i(x_j)]$ is the unknown stream function $(i, j = 1, 2, 3)$, Ω is the flow domain $(x_i^- \le x_i \le x_i^+)$ with surface

S that is characterized by a unit outer normal vector $\boldsymbol{n}$, $\Pi_v = \int T dH$ is the viscoelastic potential, T is the shear stress intensity, H is the shear strain rate intensity.

The principle (2) was proved under the following constraints:

- each component of the unknown function depends on two coordinates $\boldsymbol{\Psi} = [\psi_1(x_2, x_3), \psi_2(x_1, x_3), \psi_3(x_1, x_2)]$;
- the non-Newtonian properties of the fluid are satisfied by the Herschel-Bulkley model [34], [35];
- the unknown $\boldsymbol{\Psi}$ function and its first, second, and third partial derivatives are fixed on the surface S of the flow domain Ω.

The last point is equivalent to the boundary conditions [1], and it may have some alternative formulations [33].

The integrand (2) can be expressed in terms of the unknown $\boldsymbol{\Psi}$ function. The shear strain rate intensity H [1]:

$$H = \sqrt{2\xi_{ij}\xi_{ij}}, \tag{3}$$

depends on the components of the strain rate tensor $\mathbf{T}_\xi = [\xi_{ij}]$ that can be calculated using Cauchy's formula [32], [36], [37]:

$$\mathbf{T}_\xi = (\nabla \otimes \mathbf{V} + \mathbf{V} \otimes \nabla)/2, \tag{4}$$

where $\boldsymbol{V} = [v_i]$ is the velocity, $\nabla \otimes \mathbf{V}$ is the gradient of a vector function with components $\partial v_j / \partial x_i$.

The generalized Newtonian hypothesis is a rheological expression that allows connection of the statics and the kinematics of the fluid flow [16]:

$$T = \mu H, \tag{5}$$

where μ is the viscosity.

The Herschel-Bulkley law [34], [35] is taken into account in (2) as the rheological model of non-Newtonian fluids:

$$\mu(H) = q_0 + q_1 H^{z-1}, \tag{6}$$

where q_0, q_1, z are the parameters obtained from rheological tests.

Finally, the velocity $\boldsymbol{V}$ is a vorticity of the unknown $\boldsymbol{\Psi}$ function:

$$\mathbf{V} = \nabla \times \Psi. \tag{7}$$

In general, the 3D velocity distribution (7) depends on 3 2D scalar functions that are the components of the $\boldsymbol{\Psi}$ function. It should be noted, that the velocity distribution is solenoidal:

$$\nabla \cdot \boldsymbol{V} = \nabla \cdot (\nabla \times \boldsymbol{\Psi}) \equiv 0. \tag{8}$$

According to (8) the incompressibility condition [36], [37] is true, that makes any $\boldsymbol{\Psi}$ function kinematically admissible in the flow domain. The $\boldsymbol{\Psi}$ function is constrained on the surface S of the flow domain Ω. Since the flow rate can be expressed in terms of the stream function:

That allows to take the boundary conditions into account

[1]The Einstein summation notation is used in this work.

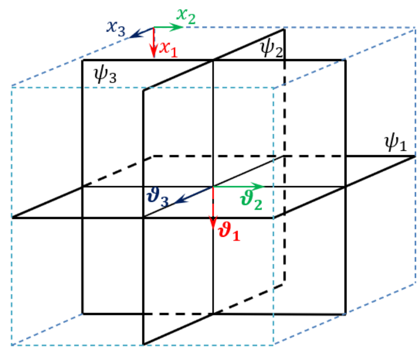

Fig. 1: The unknown stream function $\boldsymbol{\Psi}$ and the velocity function $\boldsymbol{V}$ (7) in the flow domain ($x_i^- \leq x_i \leq x_i^+$).

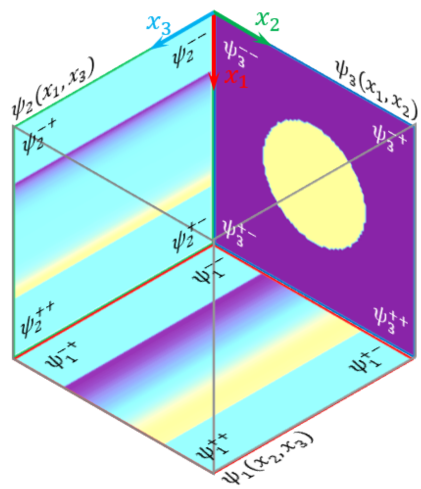

Fig. 2: The unknown stream function $\boldsymbol{\Psi}$ intuition and its values $\psi_i^{--}, \psi_i^{-+}, \psi_i^{+-}, \psi_i^{++}$ at the vertices of the the flow domain ($x_i^- \leq x_i \leq x_i^+$).

B. Numerical differentiation and integration

The following templates are applied for the numerical differentiation...

The following methods are used for the numerical intergation...

V. Simulation Modeling

The proposed loss function (2) is general and can be applied for a three-dimensional flow (7) with unknown vector function $\boldsymbol{\Psi}$, and can be implemented by means of various approaches of simulation modeling. In general, the unknown $\boldsymbol{\Psi}$ function and its first partial derivatives should have fixed values on the surface of the flow domain. Alternatively, the limitations (**??**),(**??**) should be met.

Two approaches for the implementation of the proposed physics-based loss to steady incompressible fluid flow modeling are given below. The approaches differ in a kind of applied neural network and in the method of the flow domain representation.

A. Asymptotic case: Newtonian fluid flow through a pipe

It is supposed that the Newtonian fluid flows through a cylindrical pipe with radius R. The flow is laminar and steady, the Reynolds number is smaller than the critical one $Re < Re^{*}\approx 1100...1400$ and the pipe length is greater than the critical one $L_3 > 0.16RRe$. Then the task is known as Poiseuille flow, and it has a simple analytical solution given in cylindrical coordinates $[\rho, \theta, x_3]$ [32]:

$$v_3 = -\frac{1}{4\mu}\frac{\partial p}{\partial x_3}(R^2 - \rho^2), \tag{9}$$

where $\partial p/\partial x_3$ is the pressure drop along the x_3 axis.

The flow rate trough the pipe cross section S_3 is equal to [32]:

$$Q_3 = \iint_{S_3} v_3 \rho \, d\rho \, d\theta = -\frac{\pi}{8}\frac{\partial p}{\partial x_3}\frac{R^4}{\mu}. \tag{10}$$

B. Multilayer perceptron and grid-based flow domain

The first proposed approach deals with .

C. Convolutional network and image-based flow domain

The network receives the data on the flow domain in a form of masked image of initial distribution of the unknown $\mathbf{\Psi}$ function. ...

The output of the network has the form of masked image for corrected distribution of the $\mathbf{\Psi}$ function. The following calculations with differenciations and integration operations should be done to calculate the loss and to finish the forward pass of the network.

For any given function $\mathbf{\Psi} = [\psi_i]$ that has fixed values on the boundaries of the flow domain together with its first, second, and third derivatives, the velocity distribution (7) can be expressed in compact or in expanded form, respectively:

$$\boldsymbol{V} = \left[\epsilon_{ijk}\frac{\partial \psi_k(x_i,x_j)}{\partial x_j}\right], \tag{11}$$

where ϵ_{ijk} is the Levi-Civita symbol [38],

$$\boldsymbol{V} = \left[\frac{\partial \psi_3}{\partial x_2} - \frac{\partial \psi_2}{\partial x_3}, \quad \frac{\partial \psi_1}{\partial x_3} - \frac{\partial \psi_3}{\partial x_1}, \quad \frac{\partial \psi_2}{\partial x_1} - \frac{\partial \psi_1}{\partial x_2}\right]. \tag{12}$$

It is convenient to present the flow domain Ω in the form of a parallelepiped (see Fig. 1). Then the flow rate through a cross-section $x_i = const$ can be expressed as follows:

$$Q_i(x_i) = -\epsilon_{ijk}(\psi_j(x_i, x_k^+) - \psi_j(x_i, x_k^-)l_j, \tag{13}$$

where $l_j = (x_j^+ - x_j^-)$.

The flow rates Q_i^-, Q_i^+ through 6 edges $(x_i = x_i^-, x_i = x_i^+)$ should be given as a boundary conditions, and their sum should be zero in accordance with the fluid incompressibility condition. Taking (13) into account, the flow rate balance takes the following form:

$$\begin{aligned}
Q_1(x_1^-) &= -(\psi_2^{-+} - \psi_2^{--})l_2 + (\psi_3^{-+} - \psi_3^{--})l_3,\\
Q_1(x_1^+) &= -(\psi_2^{++} - \psi_2^{+-})l_2 + (\psi_3^{++} - \psi_3^{+-})l_3,\\
Q_2(x_2^-) &= -(\psi_3^{+-} - \psi_3^{--})l_3 + (\psi_1^{-+} - \psi_1^{--})l_1,\\
Q_2(x_2^+) &= -(\psi_3^{++} - \psi_3^{-+})l_3 + (\psi_1^{++} - \psi_1^{+-})l_1,\\
Q_3(x_3^-) &= -(\psi_1^{+-} - \psi_1^{--})l_1 + (\psi_2^{+-} - \psi_2^{--})l_2,\\
Q_3(x_3^+) &= -(\psi_1^{++} - \psi_1^{-+})l_1 + (\psi_2^{++} - \psi_2^{-+})l_2.
\end{aligned} \tag{14}$$

The system linear equations (16) is redefined since 6 equations have 12 unknowns. Some additional conditions are required. For example, it is permissible to suppose that the $\mathbf{\Psi}$ has constant values on some edges of the flow domain:

$$\psi_i^{-+} = \psi_i^{--}, \psi_i^{++} = \psi_i^{+-}. \tag{15}$$

The joined system of equations (16) and (15) is closed and the boundary values of the unknown function $\mathbf{\Psi}$ at the vertices of the flow domain can be determined if the values of the flow rates $Q_i(x_i^-)$, $Q_i(x_i^+)$ (16) through the edges of the flow domain $x_i = x_i^-$, $x_i = x_i^+$ are given.

Flow rates through the edges of the flow domain:

$$\begin{aligned}
Q_1(x_1^-) &= -(\psi_2^{-+} - \psi_2^{--})l_2,\\
Q_1(x_1^+) &= -(\psi_2^{++} - \psi_2^{+-})l_2 + (\psi_3^{++} - \psi_3^{+-})l_3,\\
Q_2(x_2^-) &= -(\psi_3^{+-} - \psi_3^{--})l_3 + (\psi_1^{-+} - \psi_1^{--})l_1,\\
Q_2(x_2^+) &= -(\psi_3^{++} - \psi_3^{-+})l_3 + (\psi_1^{++} - \psi_1^{+-})l_1,\\
Q_3(x_3^-) &= -(\psi_1^{+-} - \psi_1^{--})l_1 + (\psi_2^{+-} - \psi_2^{--})l_2,\\
Q_3(x_3^+) &= -(\psi_1^{++} - \psi_1^{-+})l_1 + (\psi_2^{++} - \psi_2^{-+})l_2.
\end{aligned} \tag{16}$$

It is convenient to suppose that $\psi_j(x_i, x_k^-) = 0$, then the flow rates through the edges S_i^+ are:

$$\begin{aligned}
Q_1(x_1^-) &= -\psi_2(x_1^-, x_3^+)l_2 + \psi_3(x_1^-, x_2^+)l_3,\\
Q_1(x_1^+) &= -\psi_2(x_1^+, x_3^+)l_2 + \psi_3(x_1^+, x_2^+)l_3,\\
Q_2(x_2^-) &= -\psi_3(x_1^+, x_2^-)l_3 + \psi_1(x_2^-, x_3^+)l_1,\\
Q_2(x_2^+) &= -\psi_3(x_1^+, x_2^+)l_3 + \psi_1(x_2^+, x_3^+)l_1,\\
Q_3(x_3^-) &= -\psi_1(x_2^+, x_3^-)l_1 + \psi_2(x_1^+, x_3^-)l_2,\\
Q_3(x_3^+) &= -\psi_1(x_2^+, x_3^+)l_1 + \psi_2(x_1^+, x_3^+)l_2.
\end{aligned} \tag{17}$$

Taking into account the symmetry of the shear rate tensor $\xi_{i,j} = \xi_{i,j}$, the tensor has the following form (4):

$$\boldsymbol{T}_\xi = \frac{1}{2}\begin{bmatrix}
2\frac{\partial v_1}{\partial x_1}, & \frac{\partial v_1}{\partial x_2} - \frac{\partial v_2}{\partial x_1}, & \frac{\partial v_1}{\partial x_3} - \frac{\partial v_3}{\partial x_1}\\
\frac{\partial v_1}{\partial x_2} - \frac{\partial v_2}{\partial x_1}, & 2\frac{\partial v_2}{\partial x_2}, & \frac{\partial v_2}{\partial x_3} - \frac{\partial v_3}{\partial x_2}\\
\frac{\partial v_1}{\partial x_3} - \frac{\partial v_3}{\partial x_1}, & \frac{\partial v_2}{\partial x_3} - \frac{\partial v_3}{\partial x_2}, & 2\frac{\partial v_3}{\partial x_3}
\end{bmatrix}. \tag{18}$$

In the general case of a three dimensional flow the shear strain rate intensity H depends on all the components of the shear rate tensor:

$$H = \sqrt{2(\xi_{11}^2 + \xi_{22}^2 + \xi_{33}^2 + 2\xi_{12}^2 + 2\xi_{13}^2 + 2\xi_{23}^2)}. \tag{19}$$

Taking Newton's law of viscosity (5) and the Herschel-Bulkley law (6) into account, the loss (2) can be presented in the following form:

$$J_L^* = \iiint (\frac{q_0}{2}H^2 + \frac{q_1}{z+1}H^{z+1})\, dx_1\, dx_2\, dx_3. \tag{20}$$

TABLE II: Fragment of the validation results

degree	mean_error			
	$m = 20$		$m = 35$	
	$l_{hid} = 10$	$l_{hid} = 20$	$l_{hid} = 10$	$l_{hid} = 20$
1	0.3495	0.2887	0.2986	0.2746
2	0.0872	0.0827	0.0919	0.0828
3	0.0231	0.0230	0.0239	0.0240
4	0.0230	0.0230	0.0239	0.0239
5	0.0229	0.0230	0.0239	0.0239
6	0.0230	0.0230	0.0239	0.0238

Among all admissible $\mathbf{\Psi}$ functions, the true one gives the loss (20) minimum value. It can be seen from (12), (18), (19), (20) that the loss (20) depends on the $\mathbf{\Psi}$ function and it can be determined by means of differentiation and integration operations. The network outputs the $\mathbf{\Psi}$ function in the discrete form of a three dimensional tensor and the elements of the tensor correspond to the intensities of 3D image pixels. So, numerical differentiation and integration should be met.

The unknown $\mathbf{\Psi}$ function in (**??**) is represented in the form of a three-dimensional tensor.

where Ω is flow domain (volume) with surface S that is characterized by a unit outer normal vector $\mathbf{n}$, $\Pi_v = \int T dH$ is viscoelastic potential, $T = \sqrt{s_{ij}s_{ij}/2}$ is shear stress intensity, $H = \sqrt{2\xi_{ij}\xi_{ij}}$ is shear strain rate intensity, σ^n is total external stress on the surface S.

VI. Results and discussion

The section deals with two approaches for the implementation of the proposed physics-based loss using machine learning and study some relatively simple problems in comparison with the known analytical or numerical solutions.

A. Multilayer perceptron and grid-based flow domain

The validation process of the model is represented by a numerical experiment with different values of hyperparameters. Table II presents a fragment of a computational experiment, the values of hyperparameters varied as follows $d = [1, 2, \ldots 6]$, $l_{hid} = [10, 20, 30]$, $m = [20, 35, 50]$.

The experiment plan is a complete factorial experiment on the values of

B. Convolutional network and image-based flow domain

The previous subsection demonstrates that the proposed physics-based loss allow non-Newtonian fluid flows modelling.

TABLE III: Comparative simulation results

Method	Maximum velocity, m/s		
	parallel plates	*parallel plates with notch*	*nailfold capillary*
Analytical solution	7.5	-	-
Ansys Fluent	7.42	7.83	-
UNet with loss (**??**)	7.35	7.52	$8.8 \cdot 10^{-3}$

In the end of the section and the paper, the following advantages and disadvantages of the proposed grid-based and image-based approaches to solution of the CFD problems using ANNs in comparison with known methods in CFD should be highlighted.

Advantages.The proposed approaches are

- able to take into account the non-Newtonian properties of fluids and mass forces, e.g. magnetic force, gravity force;
- free of data sets at the training stage due to the proposed physics-based loss;
- easy in implementation, especially the image-based approach that solves a problem using an image as input;

Disadvantages. The proposed approaches are

- able to model stationary or quasi-stationary flows only;
- are time consuming and less accurate in comparison with ANSYS Fluent, at least at the present stage of using the simplest methods for approximation.

The model (2) has the following assumptions:

- able to model stationary or quasi-stationary flows only;
- are time consuming and less accurate in comparison with ANSYS Fluent, at least at the present stage of using the simplest methods for approximation.

The model (2) has the following prospects:

- able to model stationary or quasi-stationary flows only;
- are time consuming and less accurate in comparison with ANSYS Fluent, at least at the present stage of using the simplest methods for approximation.

VII. Conclusions

Complex flow domains with internal walls, porous media.

This research highlights the scope of non-Newtonian fluids flow modeling. The following conclusions should be made.

1. The proposed generalized Lagrange variational principle takes into account complex rheological properties of fluids and external body forces that allow modelling non-Newtonian and rheomagnetic fluid flows for a wide range of applications in engineering, medicine, chemistry etc. The principle is also less demanding of boundary conditions than the basic Lagrange principle.

2. The proposed generalized Lagrange functional performs a physics-based loss for machine learning algorithms. The loss minimisation does not require any data set and can be implemented in many ways. The paper demonstrates two approaches connected with grid-based and image-based flow domain representation. The second one allows modeling fluid flows using the flow domain image as input.

3. The proposed loss is mathematically justified and the obtained simulation modeling results demonstrated that the proposed algorithms are accurate enough. The algorithms can be generalized for the modeling of 3D non-Newtonian fluids flows. They also can be enhanced with more advanced methods of discretization and approximation, with application of other types of network architectures.

The authors suppose that the main prospect of the research is connected with medical applications and modeling of physiological fluid flows, including joints lubrication, blood circulation, and drug delivery tasks, using 2D and 3D images of the flow domains.

ACKNOWLEDGMENT

The authors express gratitude to the organizing committee of the IEEE 2023 Congress on Evolutionary Computation for the opportunity to discuss the results of the research, to the reviewers and the editors who helped to enhance the paper, and to Vera Panyushkina for the assistance with the translation of this paper.

AUTHORS CONTRIBUTION

Alexey Kornaev proposed Elena Kornaeva proposed in section 5 of the paper Nikita Litvinenko Ivan Stebakov Yuri Kazakov

CHECK LIST

- check if the paper is anonymous (authors, acknowledgements, contributions)
- check if there any italic Greek characters left
- read the text
- comment on this list

REFERENCES

[1] I. M. Gelfand and S. V. Fomin, *Calculus of Variations*, R. Silverman, Ed. Courier Corporation, 2000. [Online]. Available: https://books.google.com/books/about/Calculus_of_Variations.html?hl=ruid=YkFLGQeGRw4C

[2] N. Thuerey, P. Holl, M. Mueller, P. Schnell, F. Trost, and K. Um, *Physics-based Deep Learning*. WWW, 2021. [Online]. Available: http://physicsbaseddeeplearning.org

[3] X. Jin, P. Cheng, W. L. Chen, and H. Li, "Prediction model of velocity field around circular cylinder over various reynolds numbers by fusion convolutional neural networks based on pressure on the cylinder," *Physics of Fluids*, vol. 30, p. 047105, 4 2018. [Online]. Available: https://aip.scitation.org/doi/abs/10.1063/1.5024595

[4] R. Han, Y. Wang, Y. Zhang, G. C. P. of Fluids, and undefined 2019, "A novel spatial-temporal prediction method for unsteady wake flows based on hybrid deep neural network," *Physics of Fluids*, vol. 31, p. 127101, 12 2019. [Online]. Available: https://sci-hub.do/https://aip.scitation.org/doi/abs/10.1063/1.5127247

[5] P. A. Srinivasan, L. Guastoni, H. Azizpour, P. Schlatter, and R. Vinuesa, "Predictions of turbulent shear flows using deep neural networks," *Physical Review Fluids*, vol. 4, 5 2019.

[6] Y. Li, J. Chang, C. Kong, and W. Bao, "Recent progress of machine learning in flow modeling and active flow control," *Chinese Journal of Aeronautics*, vol. 35, pp. 14–44, 4 2022.

[7] K. Zubov, Z. McCarthy, Y. Ma, F. Calisto, V. Pagliarino, S. Azeglio, L. Bottero, E. Luján, V. Sulzer, A. Bharambe, N. Vinchhi, K. Balakrishnan, D. Upadhyay, and C. Rackauckas, "Neuralpde: Automating physics-informed neural networks (pinns) with error approximations," *ArXiv*, vol. abs/2017.09443, 7 2021. [Online]. Available: https://arxiv.org/abs/2107.09443v1

[8] M. Raissi, P. Perdikaris, and G. E. Karniadakis, "Physics-informed neural networks: A deep learning framework for solving forward and inverse problems involving nonlinear partial differential equations," *Journal of Computational Physics*, vol. 378, pp. 686–707, 2 2019.

[9] S. K. Mitusch, S. W. Funke, and M. Kuchta, "Hybrid fem-nn models: Combining artificial neural networks with the finite element method," *Journal of Computational Physics*, vol. 446, p. 110651, 12 2021.

[10] K. Champion, B. Lusch, J. N. Kutz, and S. L. Brunton, "Data-driven discovery of coordinates and governing equations," *Proceedings of the National Academy of Sciences of the United States of America*, vol. 116, pp. 22 445–22 451, 11 2019. [Online]. Available: https://www.pnas.org/content/116/45/22445 https://www.pnas.org/content/116/45/22445.abstract

[11] S. L. Brunton, J. L. Proctor, and J. N. Kutz, "Discovering governing equations from data by sparse identification of nonlinear dynamical systems," *Proceedings of the National Academy of Sciences*, vol. 113, no. 15, pp. 3932–3937, 2016. [Online]. Available: https://www.pnas.org/content/113/15/3932

[12] F. Sun, Y. Liu, and H. Sun, "Physics-informed spline learning for nonlinear dynamics discovery," in *Proceedings of the Thirtieth International Joint Conference on Artificial Intelligence (IJCAI-21)*, 2021, pp. 2054–2061.

[13] K. Hornik, M. Stinchcombe, and H. White, "Multilayer feedforward networks are universal approximators," *Neural Networks*, vol. 2, pp. 359–366, 1 1989.

[14] M. W. Dissanayake and N. Phan-Thien, "Neural-network-based approximations for solving partial differential equations," *Communications in Numerical Methods in Engineering*, vol. 10, pp. 195–201, 3 1994. [Online]. Available: https://onlinelibrary.wiley.com/doi/full/10.1002/cnm.1640100303

[15] E. Samaniego, C. Anitescu, S. Goswami, V. M. Nguyen-Thanh, H. Guo, K. Hamdia, T. Rabczuk, and X. Zhuang, "An energy approach to the solution of partial differential equations in computational mechanics via machine learning: Concepts, implementation and applications," *Computer Methods in Applied Mechanics and Engineering*, vol. 362, 8 2019. [Online]. Available: http://arxiv.org/abs/1908.10407 http://dx.doi.org/10.1016/j.cma.2019.112790

[16] A. Sequeira, *Hemorheology: Non-newtonian constitutive models for blood flow simulations*. Springer Verlag, 2018, vol. 2212, pp. 1–44.

[17] O. K. Baskurt, M. Boynard, G. C. Cokelet, P. Connes, B. M. Cooke, S. Forconi, F. Liao, M. R. Hardeman, F. Jung, H. J. Meiselman, G. Nash, N. Nemeth, B. Neu, B. Sandhagen, S. Shin, G. Thurston, and J. L. Wautier, "New guidelines for hemorheological laboratory techniques," *Clin. Hemorheol. Microcirc.*, vol. 42, pp. 75–97, 2009.

[18] R. Revellin, F. Rousset, D. Baud, and J. Bonjour, "Extension of murray's law using a non-newtonian model of blood flow," *Theor. Biol. Medical Model.*, vol. 6, 2009.

[19] M. M. Molla and M. C. Paul, "Les of non-newtonian physiological blood flow in a model of arterial stenosis," *Med. Eng. Phys.*, vol. 34, pp. 1079–1087, 2012.

[20] J. M. Jung, D. H. Lee, and Y. I. Cho, "Non-newtonian standard viscosity fluids," *Int. Commun. Heat Mass Transf.*, vol. 49, pp. 1–4, 2013.

[21] P. K. Mandal, "An unsteady analysis of non-newtonian blood flow through tapered arteries with a stenosis," *Int. J. Non-Linear Mech.*, vol. 40, pp. 151–164, 1 2005.

[22] E. Nader, S. Skinner, M. Romana, R. Fort, N. Lemonne, N. Guillot, A. Gauthier, S. Antoine-Jonville, C. Renoux, M. Hardy-Dessources, E. Stauffer, P. Joly, Y. Bertrand, and P. Connes, "Blood rheology: Key parameters, impact on blood flow, role in sickle cell disease and effects of exercise," *Front. Physiol.*, vol. 10, p. 1329, 2019.

[23] P. Connes, T. Alexy, J. Detterich, M. Romana, M. D. Hardy-Dessources, and S. K. Ballas, "The role of blood rheology in sickle cell disease," *Blood Reviews*, vol. 30, pp. 111–118, 3 2016.

[24] O. K. Baskurt and H. J. Meiselman, "Blood rheology and hemodynamics," *Semin. Thromb. Hemost.*, vol. 29, pp. 435–450, 2003.

[25] T. Sochi, "Non-newtonian rheology in blood circulation," pp. 1–26, 2013. [Online]. Available: http://arxiv.org/abs/1306.2067

[26] T. Bodnar, A. Sequeira, and M. Prosi, "On the shear-thinning and viscoelastic effects of blood flow under various flow rates," *Appl. Math. Comput.*, vol. 217, pp. 5055–5067, 2011.

[27] F. Abraham, M. Behr, and M. Heinkenschloss, "Shape optimization in steady blood flow: A numerical study of non-newtonian effects," *Computer Methods in Biomechanics and Biomedical Engineering*, vol. 8, pp. 127–137, 2005.

[28] Y. H. Kim, P. J. VandeVord, and J. S. Lee, "Multiphase non-newtonian effects on pulsatile hemodynamics in a coronary artery," *International Journal for Numerical Methods in Fluids*, vol. 58, pp. 803–825, 11 2008.

[29] C. Fisher and J. S. Rossmann, "Effect of non-newtonian behavior on hemodynamics of cerebral aneurysms," *Journal of Biomechanical Engineering*, vol. 131, 9 2009.

[30] J. Zueco and O. Beg, "Network$_{n}umerical_{s}imulation_{a}pplied_{t}o_{p}ulsatile''_{,}$ *Int. J. of* -16, 2009.

[31] E. Kornaeva, A. Kornaev, and S. Egorov, "Application of artificial neural networks to solution of variational problems in hydrodynamics," *Journal of Physics: Conference Series*, vol. 1553, 5 2020.

[32] L. M. Milne-Thomson and N. Rott, "Theoretical hydrodynamics, fifth edition," *Journal of Applied Mechanics*, vol. 35, pp. 846–846, 1968.

[33] E. Kornaeva, A. Kornaev, A. Fetisov, I. Stebakov, and B. Ibragimov, "Physics-based loss and machine learning approach in application to non-newtonian fluids flow modeling," *2022 IEEE Congress on Evolutionary Computation, CEC 2022 - Conference Proceedings*, 2022.

[34] L. Zheng and X. Zhang, "Exact analytical solutions for fractional viscoelastic fluids," *Modeling and Analysis of Modern Fluid Problems*, pp. 279–359, 1 2017.

[35] G. Lu, X. D. Wang, and Y. Y. Duan, "A critical review of dynamic wetting by complex fluids: From newtonian fluids to non-newtonian fluids and nanofluids," *Advances in Colloid and Interface Science*, vol. 236, pp. 43–62, 10 2016.

[36] S. V. Patankar, *Numerical Heat Transfer and Fluid Flow*, 1st ed. CRC Press, 10 1980. [Online]. Available: https://www.taylorfrancis.com/books/mono/10.1201/9781482234213/numerical-heat-transfer-fluid-flow-suhas-patankar

[37] D. Rubin and E. Krempl, *Introduction to Continuum Mechanics*, 4th ed. Elsevier Inc., 2010.

[38] G. Korn and T. Korn, *Mathematical Handbook for Scientists and Engineers*. Dover Publications, 2000.